Accuracy optimization of combined multiparameter measuring systems with application to polarized light microscopy

Mykhailo Kuian, Lothar Reichel, and Sergij V. Shiyanovskii

Phys. Rev. E **97**, 063305 — Published 25 June 2018

DOI: 10.1103/PhysRevE.97.063305

Accuracy optimization of combined multi-parameter measuring systems with application to polarized light microscopy

Mykhailo Kuian[1], Lothar Reichel[2], Sergij V. Shiyanovskii[3]

[1]*Department of Mathematical Sciences, Kent State University, Kent, OH 44242, USA, e-mail: mkuian@kent.edu*

[2]*Department of Mathematical Sciences, Kent State University, Kent, OH 44242, USA, e-mail: reichel@math.kent.edu*

[3]*Liquid Crystal Institute, Kent State University, Kent, OH 44242, USA, e-mail: sshiyano@kent.edu*

Abstract:

We study the accuracy of combined multi-parameter measuring systems (CMPMSs) that determine several unknown quantities from measurements of a single variable at different preprogrammed conditions determined by control parameters. To reduce inaccuracies of determined quantities, we propose a mathematical method for selection of control parameters that are optimal for all possible values of determined quantities. Using the submultiplicativity of the spectral and Frobenius matrix norms, we construct the upper bound of the error function and determine the set of control parameters by minimizing this bound. To demonstrate the capability of our method for CMPMSs, we apply it to the polarized light microscopy technique called LC-PolScope, which is used for determining inhomogeneous two-dimensional fields of optical retardation and orientation of optical axis in thin organic and inorganic samples. We compare the computed set of control parameters with other sets, including the one used in the PolScope, and demonstrate that our choice of control parameters works very well even though it does not take into account any specific features of the PolScope. We expect that our method will be successful in various CMPMSs, as it is applicable to any error distribution of the control parameters and measured values.

I. INTRODUCTION

Today's state-of-the-art of experimental techniques have been greatly influenced by integration of powerful computers in the experimental setups used in microscopy, tomography,

material science, biology, etc. A computer in a measuring system can have several functions. First, it can provide fast real-time calculations that mitigate disadvantages of indirect measurements, when an unknown quantity λ is determined from a measured value b through the measuring function $\Phi(\lambda)=b$. Second, it allows one to perform simultaneous measurements when several unknown quantities $\boldsymbol{\Lambda}=[\lambda_1,...,\lambda_n]$ are determined from the measurements of the same or larger, number of different physical quantities $\boldsymbol{b}=[b_1,...,b_{\bar{n}}]$ by solving a system of equations $\Phi_i(\boldsymbol{\Lambda})=b_i$ possibly in the least square sense, see e.g. [1]. Third, the computer can control and change measuring conditions. In this case one can build a CMPMS, where several stationary or slowly changing unknown quantities $\boldsymbol{\Lambda}=[\lambda_1,...,\lambda_n]$ can be determined unit by measuring a single physical variable at preprogrammed different conditions, defined by control parameter(s) $\boldsymbol{A}_i$,

$$\Phi(\boldsymbol{A}_i,\boldsymbol{\Lambda})=b_i,\ i=1,...,n, \tag{1}$$

where $\boldsymbol{A}_i$ may be a scalar $\boldsymbol{A}_i=a_i$ or a $k-$dimensional vector $\boldsymbol{A}_i=[a_{i1},...,a_{ik}]$, controlled by the computer.

The problem of best estimation of unknown quantities $\boldsymbol{\Lambda}$ from a system (1) for the case of a linear measuring functions Φ were considered in [1,2] with the solution determined by the least square method.

A central problem of this paper is how to properly select the control parameters $\boldsymbol{A}=\{a_{ij}\}$, $i=1,...,n$, $j=1,...,k$. The accuracy of measured quantities $\boldsymbol{\Lambda}$ is determined not only by the accuracy of the measurements themselves, but also by the accuracy of the settings of the control parameters. The preprogrammed selection of the set of $n\times k$ values of the control parameters $\boldsymbol{A}=[\boldsymbol{A}_1,...,\boldsymbol{A}_n]$, where $\boldsymbol{A}_i=[\alpha_{i1},...,\alpha_{ik}]$, $i=1,...,n$, is complicated when the quantities $\boldsymbol{\Lambda}$ are spatial and/or temporal functions; thus an *a priory* selection should be "optimal" for all possible values of $\boldsymbol{\Lambda}$.

In this paper we consider the class of CMPMSs that are described by a separable measuring function,

$$\Phi(\boldsymbol{A}_i,\boldsymbol{\Lambda})=\sum_{j=1}^{n} m_j(\boldsymbol{A}_i)v_j(\boldsymbol{\Lambda}),\ i=1,...,n, \tag{2}$$

where m_j, v_j, $j=1,...,n$, are smooth nonlinear functions. We develop a mathematical method for selection of control parameters in such CMPMSs that are optimal for all possible values of determined quantities. Using the submultiplicativity of the spectral and Frobenius matrix norms we construct the upper bound of the error function as a product of two functions, one of which depends only on control parameters and another one depends only on unknown quantities. We determine the set of control parameters by minimizing the former function.

To demonstrate the full capability of the proposed method we were looking for an example of CMPMS, with the following features: (a) the measuring function (2) has a simple dependence

on several control parameters and unknown quantities; (b) many sets of unknown quantities are determined concurrently at the same values of control parameters; (c) the measurement errors are dependent on both the control parameters and unknown quantities, and thus cannot be minimized simultaneously at each point of the sample. As an example of such CMPMS we considered the PolScope microscope.

The PolScope (also called LC-PolScope) described in [3-5], and its advanced versions, the Exicor MicroImager (Hinds Instruments) [6], and the Phi-Viz Imaging System (Polaviz) [7] are state-of-the-art polarized light microscopy techniques. The PolScope determines the two-dimensional fields of phase retardation $\Delta(x,y)$ and of the optical axis direction $\phi(x,y)$ of thin anisotropic samples by measuring transmitted light intensity under different conditions. The PolScope is equipped with a standard set of light source, monochromatic filter, polarizers, lenses, and CCD camera. The additional variable optical retarders are inserted in the optical path, for details see section 3 and figure 1. For each point (x,y) the sample quantities $\Delta(x,y)$ and $\phi(x,y)$ are determined by measuring transmitted light intensities $b_i = I_i(x,y)$ for different settings of two variable retarders $\boldsymbol{A}_i = [\alpha_{i1}, \alpha_{i2}]$. The intensity $I_i(x,y)$ is a product of Jones matrices of individual optical elements and has the separable form (2).

We apply our method to compute the control parameters for PolScope. We compare the computed set of control parameters with other sets, including the one used in the PolScope, and demonstrate that our choice of control parameters works very well even though it does not take into account any specific features of the PolScope.

II. DETERMINATION OF CONTROL PARAMETERS FOR CMPM SYSTEMS

For separable measuring functions of the form (2), the nonlinear system (1) can be presented in matrix form

$$\boldsymbol{M}(\boldsymbol{A}) \cdot \boldsymbol{V}(\boldsymbol{\Lambda}) = \boldsymbol{b}, \tag{3}$$

where $\boldsymbol{M}(\boldsymbol{A})$ is a matrix with elements $\boldsymbol{M}_{ij} = m_j(\boldsymbol{A}_i)$, $i, j = 1,...,n$ and $\boldsymbol{V}(\boldsymbol{\Lambda})$ is a vector of functions $v_j(\boldsymbol{\Lambda})$, $j = 1,...,n$. The elements of the vectors $\boldsymbol{b}, \boldsymbol{\Lambda}$ and $\boldsymbol{A}_i$ may correspond to different physical quantities and have different dimensions. In this case, we scale the matrix $\boldsymbol{M}(\boldsymbol{A})$ and the vectors $\boldsymbol{b}$, $\boldsymbol{\Lambda}$, $\boldsymbol{A}_i$ and $\boldsymbol{V}(\boldsymbol{\Lambda})$ to make them dimensionless.

The error-vector $\boldsymbol{\delta\tilde{\Lambda}} = \boldsymbol{\Lambda}^* - \boldsymbol{\Lambda} = [\delta\lambda_1,...,\delta\lambda_n]$ has two sources: the errors caused by inaccuracies of the measuring unit, $\boldsymbol{\delta b} = \boldsymbol{b}^* - \boldsymbol{b}$ and the errors of control parameters $\boldsymbol{\delta A} = \boldsymbol{A}^* - \boldsymbol{A} = \{\delta\alpha_{ij}\}$, $i = 1,...,n$, $j = 1,...,k$. Here $\boldsymbol{\Lambda}^*$, $\boldsymbol{A}_i^*$ and b_i^* are the true error-free values that obey the equations $\Phi(\boldsymbol{A}_i^*, \boldsymbol{\Lambda}^*) = b_i^*$, $i = 1,...,n$ and thus can be presented in the form

$$\boldsymbol{M}(\boldsymbol{A}^*)\cdot\boldsymbol{V}(\boldsymbol{\Lambda}^*) = \boldsymbol{M}(\boldsymbol{A}+\boldsymbol{\delta A})\cdot\boldsymbol{V}(\boldsymbol{\Lambda}+\boldsymbol{\delta\tilde{\Lambda}}) = \boldsymbol{b}+\boldsymbol{\delta b}. \tag{4}$$

We establish the dependence of the unknown errors $\boldsymbol{\delta\tilde{\Lambda}}$ of the control parameters and the measurement errors using methods of perturbation analysis [8], applying first-order Taylor expansion, $\boldsymbol{V}(\boldsymbol{\Lambda}+\boldsymbol{\delta\tilde{\Lambda}}) = \boldsymbol{V}(\boldsymbol{\Lambda})+\boldsymbol{\delta V}$, where $\boldsymbol{\delta V} = \boldsymbol{D}(\boldsymbol{\Lambda})\boldsymbol{\delta\tilde{\Lambda}}$ and $\boldsymbol{D}(\boldsymbol{\Lambda})$ is the Jacobian matrix with elements $D_{ji} = \dfrac{\partial v_j(\boldsymbol{\Lambda})}{\partial\lambda_i}$, $j,i = 1,...,n$. Similarly, $\boldsymbol{M}(\boldsymbol{A}+\boldsymbol{\delta A}) = \boldsymbol{M}(\boldsymbol{A})+\boldsymbol{\delta M}$, where deviations of elements of the control matrix,

$$\boldsymbol{\delta M}_{ij} = \nabla m_j(\boldsymbol{A}_i)\cdot\boldsymbol{\delta A}_i, \tag{5}$$

are caused by the errors in the control parameters $\boldsymbol{\delta A}_i = [\delta\alpha_{i1},...,\delta\alpha_{ik}]$; here $\nabla = \left[\dfrac{\partial}{\partial\alpha_{i1}},...,\dfrac{\partial}{\partial\alpha_{ik}}\right]$ is the gradient of the control parameters. Neglecting the second order term $\boldsymbol{\delta M\delta V}$ in equation (4) and subtracting equation (3) leads to the equation

$$\boldsymbol{M}(\boldsymbol{A})\boldsymbol{\delta V}+\boldsymbol{\delta M}\boldsymbol{V}(\boldsymbol{\Lambda}) = \boldsymbol{\delta b}, \tag{6}$$

transforms into an expression for the measurement error vector:

$$\boldsymbol{\delta\tilde{\Lambda}} = \boldsymbol{D}^{-1}(\boldsymbol{\Lambda})\boldsymbol{M}^{-1}(\boldsymbol{A})\boldsymbol{\delta b} - \boldsymbol{D}^{-1}(\boldsymbol{\Lambda})\boldsymbol{M}^{-1}(\boldsymbol{A})\boldsymbol{\delta M}(\boldsymbol{A},\boldsymbol{\delta A})\boldsymbol{V}(\boldsymbol{\Lambda}). \tag{7}$$

We can scale the error vector $\boldsymbol{\delta\Lambda} = \boldsymbol{\Theta\delta\tilde{\Lambda}}$ by selecting the numerical values of $\boldsymbol{\Theta}_{ii}$, $i = 1,...,n$, based on the 'importance' of determined values λ_i; however, as one can see below, the proposed selection of the control parameters $\boldsymbol{A}$ does not depend on $\boldsymbol{\Theta}$. We measure the error vector with the Euclidian norm (length) $\|\boldsymbol{\delta\Lambda}\|_2 = \sqrt{\sum_{i=1}^{n}\delta\lambda_i^{\,2}}$. From equation (7), the vector $\boldsymbol{\delta\Lambda}$ consists of two terms, $\boldsymbol{\delta\Lambda} = \boldsymbol{\delta\Lambda}_{\boldsymbol{M}}+\boldsymbol{\delta\Lambda}_{\boldsymbol{B}}$, where the error

$$\boldsymbol{\delta\Lambda}_{\boldsymbol{M}} = \boldsymbol{\Theta D}^{-1}(\boldsymbol{\Lambda})\boldsymbol{M}^{-1}(\boldsymbol{A})\boldsymbol{\delta M}(\boldsymbol{A},\boldsymbol{\delta A})\boldsymbol{V}(\boldsymbol{\Lambda}), \tag{8}$$

is caused by errors in the setting of the control parameters, and

$$\boldsymbol{\delta\Lambda_B} = -\boldsymbol{\Theta D}^{-1}(\boldsymbol{\Lambda})\boldsymbol{M}^{-1}(\boldsymbol{A})\boldsymbol{\delta b} \tag{9}$$

stems from measurements inaccuracies. Elements of the vectors $\boldsymbol{\delta\Lambda_M}$ and $\boldsymbol{\delta\Lambda_B}$ are linear functions of respectively, $\delta\alpha_{ij}$ and δb_i, which we assume to be accidental errors , i.e. mutually independent, random zero-mean quantities:

$$E\left[\delta\alpha_{ij}\delta\alpha_{i'j'}\right] = \sigma^2(\delta\alpha_{ij})\delta_{ii'}\delta_{jj'}, \quad E\left[\delta b_j \delta b_{j'}\right] = \sigma^2(\delta b_j)\delta_{jj'}, \quad E\left[\delta\alpha_{ij}\delta b_k\right] = 0, \tag{10}$$

here E is the expectation operator and σ is the standard deviation. With this assumption we obtain the following equations:

$$E\left[\left\|\boldsymbol{\delta\Lambda}\right\|_2^2\right] = E\left[\left\|\boldsymbol{\delta\Lambda_M}\right\|_2^2\right] + E\left[\left\|\boldsymbol{\delta\Lambda_B}\right\|_2^2\right], \tag{11}$$

where

$$E\left[\left\|\boldsymbol{\delta\Lambda_M}\right\|_2^2\right] = \sum_{i,l=1}^{n}\sum_{j=1}^{k}\Theta_{ii}^2\left(\frac{\partial\lambda_i}{\partial\alpha_{lj}}\right)^2\sigma^2(\delta\alpha_{lj}), \tag{12}$$

$$E\left[\left\|\boldsymbol{\delta\Lambda_B}\right\|_2^2\right] = \sum_{i=1}^{n}\Theta_{ii}^2\left(\frac{\partial\lambda_i}{\partial b_i}\right)^2\sigma^2(\delta b_i) \tag{13}$$

define the contributions caused by the errors in the control parameters and measured values, respectively. Both functions depend on the control parameters $\boldsymbol{A}$ and on the quantities $\boldsymbol{\Lambda}$; the former are usually a single set selected before the experiment, the latter are unknown and may change during the experiment. A single set $\boldsymbol{A}$ cannot concurrently minimize the expressions $E\left[\left\|\boldsymbol{\delta\Lambda_M}\right\|_2^2\right]$, $E\left[\left\|\boldsymbol{\delta\Lambda_B}\right\|_2^2\right]$ or their sum (11) for all measured values of $\boldsymbol{\Lambda}$. Thus, we consider them separately and will minimize their upper bounds using the sub-multiplicative property of the spectral matrix norm and the linearity of the expectation operator:

$$E\left[\left\|\boldsymbol{\delta\Lambda_M}\right\|_2^2\right] = E\left[\left\|\boldsymbol{\Theta D}^{-1}(\boldsymbol{\Lambda})\boldsymbol{M}^{-1}(\boldsymbol{A})\boldsymbol{\delta M V}(\boldsymbol{\Lambda})\right\|_2^2\right] \le \left\|\boldsymbol{\Theta D}^{-1}(\boldsymbol{\Lambda})\right\|_2^2\left\|\boldsymbol{V}(\boldsymbol{\Lambda})\right\|_2^2 E\left[\left\|\boldsymbol{M}^{-1}(\boldsymbol{A})\boldsymbol{\delta M}\right\|_2^2\right], \tag{14}$$

$$E\left[\left\|\boldsymbol{\delta\Lambda_B}\right\|_2^2\right] = E\left[\left\|\boldsymbol{\Theta D}^{-1}(\boldsymbol{\Lambda})\boldsymbol{M}^{-1}(\boldsymbol{A})\boldsymbol{\delta b}\right\|_2^2\right] \le \left\|\boldsymbol{\Theta D}^{-1}(\boldsymbol{\Lambda})\right\|_2^2 E\left[\left\|\boldsymbol{M}^{-1}(\boldsymbol{A})\boldsymbol{\delta b}\right\|_2^2\right]. \tag{15}$$

The spectral matrix norm of an arbitrary matrix $\boldsymbol{W}$ is defined as $\|\boldsymbol{W}\|_2 = \sup_{\boldsymbol{x}\neq\boldsymbol{0}} \frac{\|\boldsymbol{W}\boldsymbol{x}\|_2}{\|\boldsymbol{x}\|_2}$, where $\sup_{\boldsymbol{x}\neq\boldsymbol{0}}$ denotes the smallest upper bound of the expression for all possible vectors $\boldsymbol{x}\neq\boldsymbol{0}$. To minimize (14) , we keep the factors $\left\|\boldsymbol{\Theta}\boldsymbol{D}^{-1}(\boldsymbol{\Lambda})\right\|_2^2$ and $\left\|\boldsymbol{V}(\boldsymbol{\Lambda})\right\|_2^2$, which are independent of $\boldsymbol{A}$, and bound the spectral norm in $E\left[\left\|\boldsymbol{M}^{-1}(\boldsymbol{A})\boldsymbol{\delta M}\right\|_2^2\right]$ by the Frobenius matrix norm $\left\|\boldsymbol{M}^{-1}(\boldsymbol{A})\boldsymbol{\delta M}\right\|_2^2 \le \left\|\boldsymbol{M}^{-1}(\boldsymbol{A})\boldsymbol{\delta M}\right\|_F^2$, [9], because the square of the Frobenius norm, defined as $\|\boldsymbol{W}\|_F^2 = Tr(\boldsymbol{W}^T\boldsymbol{W}) = \sum_i\sum_j \boldsymbol{W}_{ij}^2$, is easily explicitly calculated as

$$\left\|\boldsymbol{M}^{-1}(\boldsymbol{A})\boldsymbol{\delta M}\right\|_F^2 = \sum_{p=1}^{n}\sum_{s=1}^{n}\left(\sum_{i=1}^{n}\sum_{j=1}^{k}\psi_{pi}\frac{\partial m_s(\boldsymbol{A}_i)}{\partial\alpha_{ij}}\delta\alpha_{ij}\right)^2, \tag{16}$$

where $\psi_{pi} = \left[\boldsymbol{M}^{-1}(\boldsymbol{A})\right]_{pi}$ are the elements of the inverse matrix $\boldsymbol{M}^{-1}(\boldsymbol{A})$. Using equations (16) and (10), we obtain an upper bound for $E\left[\left\|\boldsymbol{\delta\Lambda}_{\boldsymbol{M}}\right\|_2^2\right]$,

$$E\left[\left\|\boldsymbol{\delta\Lambda}_{\boldsymbol{M}}\right\|_2^2\right] \le \left\|\boldsymbol{\Theta}\boldsymbol{D}^{-1}(\boldsymbol{\Lambda})\right\|_2^2\left\|\boldsymbol{V}(\boldsymbol{\Lambda})\right\|_2^2\sum_{p=1}^{n}\sum_{s=1}^{n}\sum_{i=1}^{n}\sum_{j=1}^{k}\sigma_{ij}^2(\delta\alpha_{ij})\psi_{pi}^2\left(\frac{\partial m_s(\boldsymbol{A}_i)}{\partial\alpha_{ij}}\right)^2. \tag{17}$$

If we can assume that the absolute errors $\delta\alpha_{ij}$ are identically distributed, $\sigma_{ij}^2(\delta\alpha_{ij}) = \sigma_\alpha^2$, then

$$E\left[\left\|\boldsymbol{\delta\Lambda}_{\boldsymbol{M}}\right\|_2^2\right] \le \sigma_\alpha^2\left\|\boldsymbol{\Theta}\boldsymbol{D}^{-1}(\boldsymbol{\Lambda})\right\|_2^2\left\|\boldsymbol{V}(\boldsymbol{\Lambda})\right\|_2^2 P_M^a(\boldsymbol{A}), \tag{18}$$

where

$$P_M^a(\boldsymbol{A}) = \sum_{p=1}^{n}\sum_{s=1}^{n}\sum_{i=1}^{n}\sum_{j=1}^{k}\psi_{pi}^2\left(\frac{\partial m_s(\boldsymbol{A}_i)}{\partial\alpha_{ij}}\right)^2 \tag{19}$$

is the function that governs the minimization of $E\left[\left\|\boldsymbol{\delta\Lambda}_{\boldsymbol{M}}\right\|_2^2\right]$.

If the errors in the control parameters $\delta\alpha_{ij}$ are proportional to their magnitudes α_{ij}, then $\delta\alpha_{ij}$ can be expressed as $\varepsilon\alpha_{ij}$, where ε is a random variable, $\sigma(\nu) = \sigma_\varepsilon$, $\sigma(\delta\alpha_{ij}) = \sigma_\varepsilon\alpha_{ij}$, and

$$E\left[\left\|\boldsymbol{\delta\Lambda}_{\boldsymbol{M}}\right\|_2^2\right] \le \sigma_\varepsilon^2\left\|\boldsymbol{\Theta}\boldsymbol{D}^{-1}(\boldsymbol{\Lambda})\right\|_2^2\left\|\boldsymbol{V}(\boldsymbol{\Lambda})\right\|_2^2 P_M^r(\boldsymbol{A}) \tag{20}$$

is determined by the function

$$P_M^r(\boldsymbol{A}) = \sum_{p=1}^{n}\sum_{s=1}^{n}\sum_{i=1}^{n}\sum_{j=1}^{k}\alpha_{ij}^2\psi_{pi}^2\left(\frac{\partial m_s(\boldsymbol{A}_i)}{\partial\alpha_{ij}}\right)^2. \tag{21}$$

Now, we consider the function $E\left[\|\boldsymbol{\delta\Lambda_B}\|_2^2\right]$, see equation (15), which depends on $\boldsymbol{A}$ through $E\left[\|\boldsymbol{M}^{-1}(\boldsymbol{A})\boldsymbol{\delta b}\|_2^2\right]$. If the measurement errors δb_i do not depend on b_i and are identically distributed, $\sigma(\delta b_j)=\sigma_b$, then $E\left[\|\boldsymbol{M}^{-1}(\boldsymbol{A})\boldsymbol{\delta b}\|_2^2\right] = \|\boldsymbol{M}^{-1}(\boldsymbol{A})\|_F^2\,\sigma_b^2$ and

$$E\left[\|\boldsymbol{\delta\Lambda_B}\|_2^2\right] \le \sigma_b^2\,\|\boldsymbol{\Theta D}^{-1}(\boldsymbol{\Lambda})\|_2^2\,P_b^a(\boldsymbol{A}) \tag{22}$$

is determined by the function

$$P_b^a(\boldsymbol{A}) = \|\boldsymbol{M}^{-1}(\boldsymbol{A})\|_F^2 = \sum_{i=1}^{n}\sum_{j=1}^{n}\psi_{ij}^2(\boldsymbol{A}). \tag{23}$$

If the measurement errors δb_i are proportional to b_i, then the error vector $\boldsymbol{\delta b}$ can be expressed as $\boldsymbol{\delta b}=\boldsymbol{\Xi b}$, where $\boldsymbol{\Xi}$ is a diagonal matrix with identically distributed random elements $\boldsymbol{\Xi}_{ii}$, $\sigma(\boldsymbol{\Xi}_{ii})=\sigma_\Xi$. From the equality $\boldsymbol{M}(\boldsymbol{A})\cdot\boldsymbol{V}(\boldsymbol{\Lambda})=\boldsymbol{b}$, we get

$$E\left[\|\boldsymbol{\delta b}\|_2^2\right] = E\left[\|\boldsymbol{\Xi b}\|_2^2\right] = \sigma_\Xi^2\,\|\boldsymbol{M}(\boldsymbol{A})\cdot\boldsymbol{V}(\boldsymbol{\Lambda})\|_2^2 \le \sigma_\Xi^2\,\|\boldsymbol{M}(\boldsymbol{A})\|_F^2\,\|\boldsymbol{V}(\boldsymbol{\Lambda})\|_2^2$$

and

$$E\left[\|\boldsymbol{\delta\Lambda_B}\|_2^2\right] \le \sigma_\Xi^2\,\|\boldsymbol{V}(\boldsymbol{\Lambda})\|_2^2\,\|\boldsymbol{\Theta D}^{-1}(\boldsymbol{\Lambda})\|_2^2\,P_b^r(\boldsymbol{A}), \tag{24}$$

where $P_b^r(\boldsymbol{A})$ is the condition number of $\boldsymbol{M}(\boldsymbol{A})$

$$P_b^r(\boldsymbol{A}) = cond\left(\boldsymbol{M}(\boldsymbol{A})\right) = \|\boldsymbol{M}^{-1}(\boldsymbol{A})\|_F^2\,\|\boldsymbol{M}(\boldsymbol{A})\|_F^2 = \sum_{i,j=1}^{n}\sum_{p,s=1}^{n}\psi_{ij}^2(\boldsymbol{A})\,m_{ps}^2(\boldsymbol{A}). \tag{25}$$

Using equations (18), (20), (22) and (24), one can see that the "optimal" choice of the control parameters that minimizes the upper bound for the total error (11) can be found by minimization of the weighted function

$$P_{tot}(\boldsymbol{A}) = wP_M^\xi(\boldsymbol{A}) + (1-w)P_b^\eta(\boldsymbol{A}), \tag{26}$$

where ξ and η are either a, see equations (19) and (23), or r, see equations (21) and (25), depending on whether the errors in the control parameters and the measured values are absolute or relative. The weighting coefficient $0 \le w \le 1$ is determined by the products in equations (18), (20), (22) and (24).

If the errors in the measured values b_i have relative form, see equation (24), then w is determined only by the standard deviations σ_ν and σ_Ξ,

$$w = \frac{\sigma_\nu^2}{\sigma_\nu^2 + \sigma_\Xi^2}, \tag{27}$$

where the parameter ν is either a, or ε, depending on whether the errors in the control parameters and the measured values are absolute or relative. In this case, equation (26) does not depend on the unknown quantities $\boldsymbol{\Lambda}$ and, therefore, allows one to determine the control parameters $\boldsymbol{A}$ by minimization of the function (26). If the errors in the measured values are absolute, see equation (22), then the weighting coefficient

$$w = \frac{\|\boldsymbol{V}(\boldsymbol{\Lambda})\|_2^2 \sigma_\nu^2}{\|\boldsymbol{V}(\boldsymbol{\Lambda})\|_2^2 \sigma_\nu^2 + \sigma_b^2} \tag{28}$$

depends on $\boldsymbol{\Lambda}$. Additional assumptions are required to justify the minimization of (26). If either term in the denominator of (28) is or $\|\boldsymbol{V}(\boldsymbol{\Lambda})\|_2^2$ remains almost constant in the domain of possible values of $\boldsymbol{\Lambda}$, then one may assume w to be constant and minimize (26). In the case when w in (28) strongly depends on $\boldsymbol{\Lambda}$, we propose the following procedure, which is similar to single parameter optimization. For several selected values of w, we calculate the corresponding "optimal" sets $\boldsymbol{A}$ by minimizing the function (26), and between them choose the best set by comparing the total error functions (11). Further refinement of w can be performed if necessary.

To summarize, the goal of our method is to construct an effective error function (26), which does not depend on unknown quantities and is an upper bound for the true error function (11). We then minimize function (26) and determine the optimal set of control parameters $\boldsymbol{A}$. Below we demonstrate how the proposed method is implemented for PolScope.

III. APPLICATION OF THE PROPOSED METHOD TO THE POLSCOPE

In this section we apply the proposed method to PolScope [3,4,10]. PolScopes are widely used to study patterns with submicron resolution in various inhomogeneous anisotropic films, in particular, biological cells, polymer samples, liquid crystal films, etc. The PolScope is a polarized light microscope, where a quarter-wave plate and two liquid crystal (LC) variable optical retarders LCA and LCB, see figure 1, are added to a standard set of optical elements: light source, monochromatic filter, polarizer, lenses, analyzer and CCD camera. The PolScope determines in-plane, two-dimensional fields of phase retardance $\Delta(x,y)$ and of the azimuth $\phi(x,y)$ of slow optic axis from a sequence of measurements of transmitted light intensity obtained for the different retardances of LCA and LCB set by the computer controlled applied voltages. The phase retardance $\Delta(x,y)$ and azimuth $\phi(x,y)$ are determined by the four-frame algorithm [3,4,10]. The corresponding function of the output intensity at the CCD camera I_{out} can be derived within the Jones calculus, which is an efficient technique to analyze optical devices consisting of linear non-reflecting polarization, sensitive optical elements.

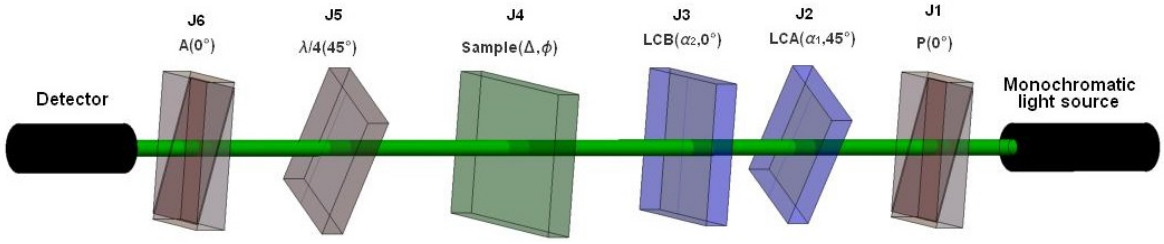

FIG. 1. (Color online) Scheme of the PolScope microscope. Liquid-crystal plates LCA and LCB have variable values of retardances, α_1 and α_2 ; $\lambda/4$ is a quarter-wave plate with phase shift between polarization components equal $\pi/2$, *P* and *A* are the linear polarizer and analyzer transmit only horizontal component of the beam.

The basic elements of the Jones calculus is the 2D Jones vector $\mathbf{j}=\begin{bmatrix} E_x \\ E_y \end{bmatrix}$, which is the complex amplitude of the electric field $\mathbf{E}=\mathbf{j}\exp\left(2\pi i(z-ct)/\lambda\right)$ of the plane monochromatic wave with the wavelength λ, and the 2×2 Jones matrix of an optical element $\mathbf{J}$ that defines the transformation of the Jones vector $\mathbf{j}_{\text{out}} = \mathbf{J}\,\mathbf{j}_{\text{in}}$ [11]. The optical scheme of the PolScope system, shown on figure 1, contains two types of optical elements: linear polarizers and phase retarders.

The Jones matrix of a linear polarizer, which transmits horizontal polarization along the Ox axis, is $\mathbf{J_H} = \begin{bmatrix} 1 & 0 \\ 0 & 0 \end{bmatrix}$. The Jones matrix of a phase retarder is defined by its phase retardance ψ and the angle θ between its slow optic axis and the Ox axis,

$$\mathbf{J_r}(\xi,\theta) = \mathbf{R}(-\theta)\mathbf{J_r}(\xi,0)\mathbf{R}(\theta), \tag{29}$$

where $\mathbf{J_r}(\xi,0) = \begin{bmatrix} e^{-i\xi/2} & 0 \\ 0 & e^{i\xi/2} \end{bmatrix}$ is the Jones matrix if the slow axis is parallel to Ox axis, and $\mathbf{R}(\theta) = \begin{bmatrix} \cos\theta & -\sin\theta \\ \sin\theta & \cos\theta \end{bmatrix}$ is the rotation matrix. Then, the Jones matrices of the optical elements in the PolScope are: $\mathbf{J}_1 = \mathbf{J_H}$ for the linear polarizer, $\mathbf{J}_2 = \mathbf{J_r}(\alpha_1, \pi/4)$ for the liquid-crystal variable retarder LCA rotated by $\pi/4$, $\mathbf{J}_3 = \mathbf{J_r}(\alpha_2, 0)$ for the liquid-crystal variable retarder LCB, $\mathbf{J}_4(x,y) = \mathbf{J_r}\left(\Delta(x,y), \varphi(x,y)\right)$ for the (x,y) pixel of the specimen, $\mathbf{J}_5 = \mathbf{J_r}(\pi/4, \pi/4)$ for the quarter-wave plate rotated by $\pi/4$, and $\mathbf{J}_6 = \mathbf{J_H}$ for the linear analyzer. Thus, the transmission coefficient the PolScope T_{PS} is determined by the Jones matrix $\mathbf{J}_{PS} = \mathbf{J}_6\mathbf{J}_5\mathbf{J}_4\mathbf{J}_3\mathbf{J}_2$ that transforms the normalized Jones vector after the polarizer $\mathbf{j}_{\text{in}} = \begin{bmatrix} 1 \\ 0 \end{bmatrix}$ into the Jones vector after the analyzer $\mathbf{j}_{\text{out}} = \mathbf{J}_{PS}\mathbf{j}_{\text{in}}$:

$$T_{\text{PS}} = \mathbf{j}_{\text{out}}^{*} \cdot \mathbf{j}_{\text{out}} = \frac{1}{2}\left(1 + \sin\alpha_1 \cos\alpha_2 \cos\Delta - \sin\alpha_1 \sin\alpha_2 \cos 2\phi \sin\Delta + \cos\alpha_1 \sin 2\phi \sin\Delta\right), \tag{30}$$

where $\mathbf{j}_{\text{out}}^{*}$ denotes complex conjugate of vector $\mathbf{j}_{\text{out}}$.

Considering the inhomogeneous distributions of the input intensity $I_{\text{in}}(x,y)$ and of the depolarized leakage $I_{\text{leak}}(x,y)$, one obtains the output intensity distribution at the CCD camera $I_{\text{out}}(x,y)$ as

$$I_{\text{out}} = I_{\text{leak}} + I_{\text{in}}T_{\text{PS}} = I_{\text{leak}} + \frac{1}{2}I_{\text{in}}\left(1 + \sin\alpha_1 \cos\alpha_2 \cos\Delta - \sin\alpha_1 \sin\alpha_2 \cos 2\phi \sin\Delta + \cos\alpha_1 \sin 2\phi \sin\Delta\right). \tag{31}$$

The intensity function (31) has separable form (2) and contains the four-dimensional vector of unknown quantities $\boldsymbol{\Lambda}=\left[I_{\text{leak}},I_{\text{in}},\Delta,\phi\right]^{T}$ that requires four measurements, $i=1,...,4$, of the intensity $I_{\text{out}}=I_i$ with different sets of the control parameters $\boldsymbol{A}_i=[\alpha_{i1},\alpha_{i2}]$. Thus, $\boldsymbol{\Lambda}$ is determined from equation (3) where

$$\boldsymbol{M}(\boldsymbol{A})=\begin{bmatrix}1 & \sin\alpha_{11}\cos\alpha_{12} & \sin\alpha_{11}\sin\alpha_{12} & \cos\alpha_{11}\\ 1 & \sin\alpha_{21}\cos\alpha_{22} & \sin\alpha_{21}\sin\alpha_{22} & \cos\alpha_{21}\\ 1 & \sin\alpha_{31}\cos\alpha_{32} & \sin\alpha_{31}\sin\alpha_{32} & \cos\alpha_{31}\\ 1 & \sin\alpha_{41}\cos\alpha_{42} & \sin\alpha_{41}\sin\alpha_{42} & \cos\alpha_{41}\end{bmatrix},\ \boldsymbol{V}(\boldsymbol{\Lambda})=\begin{bmatrix}I_{leak}+\frac{I_{in}}{2}\\ \frac{I_{in}\cos\Delta}{2}\\ -\frac{I_{in}\sin\Delta\cos2\phi}{2}\\ \frac{I_{in}\sin\Delta\sin2\phi}{2}\end{bmatrix},\ \boldsymbol{b}=\begin{bmatrix}I_1\\ I_2\\ I_3\\ I_4\end{bmatrix}. \quad (32)$$

In equations (8) and (9), we choose the diagonal matrix $\boldsymbol{\Theta}=diag\left[0,0,1,1\right]$ because we are not interested in values of I_{leak} and I_{in}, and the "importance" of the dimensionless quantities Δ and ϕ is assumed to be equal.

The matrix

$$\boldsymbol{\Theta D}^{-1}=\frac{1}{I_{in}}\begin{bmatrix}0 & 0 & 0 & 0\\ 0 & 0 & 0 & 0\\ 0 & 0 & -2\cos\Delta\cos2\phi & \frac{\sin2\phi}{\sin\Delta}\\ 0 & 0 & 2\cos\Delta\sin2\phi & \frac{\cos2\phi}{\sin\Delta}\end{bmatrix} \quad (33)$$

multiplies both error vectors (8) and (9). Taking into account that the depolarized leakage I_{leak} depends linearly on I_{in}, and $I_{leak}<<I_{in}$, we assume that the measuring errors do not significantly depend on I_{in} and I_{leak}. We set $I_{in}=1$, and $I_{leak}=0$. For the PolScope, the errors in the control parameters δa_{ij} are absolute, i.e. do not depend on the parameter values a_{ij}, and the measurement errors δb_i are relative, $\delta b_i=\Xi_{ii}b_i$, where $\Xi_{ii}\sim1\%$ [3]. Thus, we start the search of the set of "optimal" values of $\boldsymbol{A}$ by separately minimizing the functions (19) and (25). To determine these minima, we apply the Nelder-Mead algorithm implemented in Wolfram Mathematica. The function (19) achieves its minimum $\min P_M^a(\boldsymbol{A})=4.907$ at

$$\boldsymbol{A}=\boldsymbol{A}^{\boldsymbol{M}}=[[180^{\circ},90^{\circ}][51.36^{\circ},180^{\circ}][51.36^{\circ},0^{\circ}][91.83^{\circ},90^{\circ}]], \quad (34)$$

where for better visibility we present here and below the variable phase redardances α_1 and α_2 in degrees, rather than in radians. The function (25) reaches $\min P_b^r(\boldsymbol{A}) = 3.9051$ at

$$\boldsymbol{A} = \boldsymbol{A^B} = [[180^\circ, 90^\circ][51.58^\circ, 180^\circ][51.58^\circ, 0^\circ][93.56^\circ, 90^\circ]]. \tag{35}$$

Note that the sets $\boldsymbol{A^M}$ and $\boldsymbol{A^B}$ are almost the same, and the value $P_M^a(\boldsymbol{A^B}) = 4.909$ is close to the minimum of the function $P_M^a(\boldsymbol{A^M})$, while $P_b^r(\boldsymbol{A^M}) = 3.906$ is close to minimum of the function $P_b^r(\boldsymbol{A^B})$. Thus, the set of 'optimized' control parameters is almost independent on the weighting coefficient w in the weighted function (26) and we can choose either set of the control parameters $\boldsymbol{A^M}$ or $\boldsymbol{A^B}$. We select $\boldsymbol{A} = \boldsymbol{A^B}$ as the "optimal" set of control parameters.

To compare different sets of control parameters, we represent their values $\boldsymbol{A}_i = [\alpha_{i1}, \alpha_{i2}]$ by the Jones vector $\mathbf{j}_3 = \mathbf{J}_3\mathbf{J}_2\,\mathbf{j}_{\text{in}}$ of the light entering the sample. A linear polarizer $P(0^\circ)$ and two liquid crystal plates $LCA(\alpha_1, 45^\circ)$ and $LCA(\alpha_2, 0^\circ)$, see figure 1, form the universal compensator [10], because the variable retardance values $\alpha_1 := \alpha_{i1}$, $\alpha_2 := \alpha_{i2}$ provide the transformation of the unpolarized illumination light beam into any polarization state, with the Jones vector:

$$\mathbf{j}_3 = \left[\cos\left(\frac{\alpha_{i1}}{2}\right) e^{-i\frac{\alpha_{i2}}{2}} \quad \sin\left(\frac{\alpha_{i1}}{2}\right) e^{i\left(\frac{\alpha_{i2}}{2} - \frac{\pi}{2}\right)} \right]^T \tag{36}$$

Figure 2 shows the control parameters $\boldsymbol{A}_i = [\alpha_{i1}, \alpha_{i2}]$ and the corresponding polarization state (36) using standard representations with the Stokes parameters, S_0=1, S_1, S_2, S_3, and the Poincaré sphere, [12]:

$$\begin{aligned} S_1 &= \cos\alpha_{i1} = \cos\chi\cos\psi \\ S_2 &= \sin\alpha_{i1}\sin\alpha_{i2} = \cos\chi\sin\psi \\ S_3 &= -\sin\alpha_{i1}\cos\alpha_{i2} = \sin\chi \end{aligned} \tag{37}$$

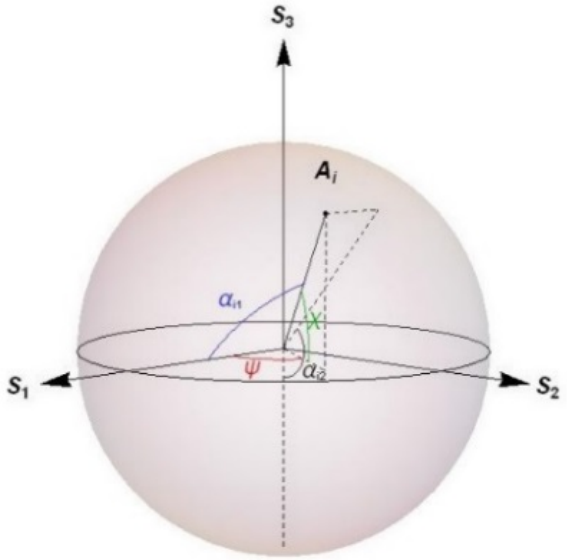

FIG. 2**.** (Color online) Representation of the control parameters of measurement $A_i = [\alpha_{i1}, \alpha_{i2}]$ through the Jones vector (36) on the Poincare sphere in the space of the Stokes parameters, S_1, S_2, S_3. χ is the ellipticity angle and ψ defines the orientation of the major axis of the polarization ellipse.

On the Poincaré sphere, right and left circular polarizations correspond to the north and south poles, respectively, and the linear polarizations lie on the equator. In the four-frame algorithm, for the samples with full range of possible retardance values the following set of control parameters was used:

$$A^{90} = [[90^\circ, 180^\circ][90^\circ - \mathrm{X}, 180^\circ][90^\circ + \mathrm{X}, 180^\circ][90^\circ, 180^\circ - \mathrm{X}]],\ \mathrm{X} = 90^\circ. \qquad (38)$$

To study biological samples, e.g. living cells, when retardance values of the sample have mostly small values, Oldenbourg and Shribak [3] proposed to use the set of control parameters:

$$A^{11} = [[90^\circ, 180^\circ][90^\circ - \mathrm{X}, 180^\circ][90^\circ + \mathrm{X}, 180^\circ][90^\circ, 180^\circ - \mathrm{X}]],\ \mathrm{X} = 10.8^\circ. \qquad (39)$$

We also examine a configuration on the Poincare sphere that is interesting from a symmetry point of view -the right tetrahedron set:

$$A^{T} = [[90^\circ, 180^\circ][30^\circ, 0^\circ][115.66^\circ, 56.3^\circ][115.66^\circ, -56.3^\circ]]. \qquad (40)$$

The polarization states of the four illumination beam settings (35), (38), (39), (40) are shown on the Poincare sphere in figure 3.

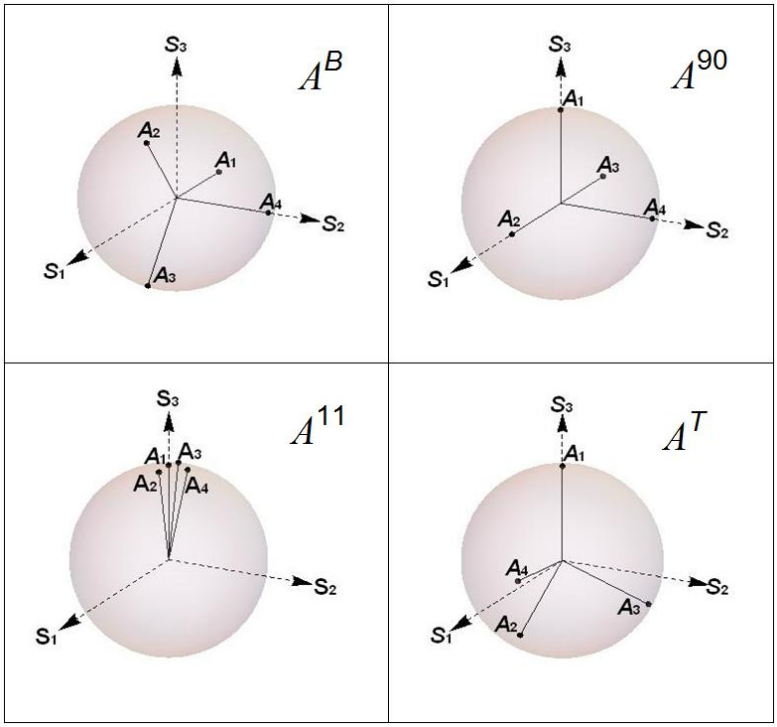

FIG. 3. (Color online) Sets of control parameters $\boldsymbol{A}^{\boldsymbol{B}}$, $\boldsymbol{A}^{\boldsymbol{90}}$, $\boldsymbol{A}^{\boldsymbol{11}}$, $\boldsymbol{A}^{\boldsymbol{T}}$ shown on the Poincare sphere.

To compare the effect of the selected control parameter sets on the measurement accuracy, we calculate the errors of phase retardance $\delta\Delta$ and azimuth of the slow optical axis $\delta\phi$ using equation (7). The errors $\delta\Delta$ and $\delta\phi$ split into the control parameters errors, $\delta\Delta_M$, $\delta\phi_M$, (8), and the measuring errors, $\delta\Delta_B$, $\delta\phi_B$, (9). Considering the control parameter errors $\boldsymbol{\delta A}=\{\delta\alpha_{ij}\}$, $i=1,..,4$, $j=1,2$, to be uniformly distributed, $\delta\alpha_{ij}\sim unif[-\sqrt{3}\sigma_\alpha,\sqrt{3}\sigma_\alpha]$ with standard deviation σ_α, we obtain from (12) the standard deviations of the propagated errors $\delta\Delta_M$ and $\delta\phi_M$,

$$\sigma(\delta\Delta_M)=\sigma_\alpha\sqrt{\sum_{i=1}^{4}\sum_{j=1}^{2}\left(\frac{\partial\Delta_M}{\partial\alpha_{ij}}\right)^2},\quad \sigma(\delta\phi_M)=\sigma_\alpha\sqrt{\sum_{i=1}^{4}\sum_{j=1}^{2}\left(\frac{\partial\phi_M}{\partial\alpha_{ij}}\right)^2}. \tag{41}$$

The normalized standard deviations $\sigma(\delta\Delta_M)/\sigma_\alpha$, $\sigma(\delta\phi_M)/\sigma_\alpha$ are shown in figure 4 as functions of Δ for several fixed values of ϕ for the set $\boldsymbol{A}=\boldsymbol{A}^{\boldsymbol{B}}$.

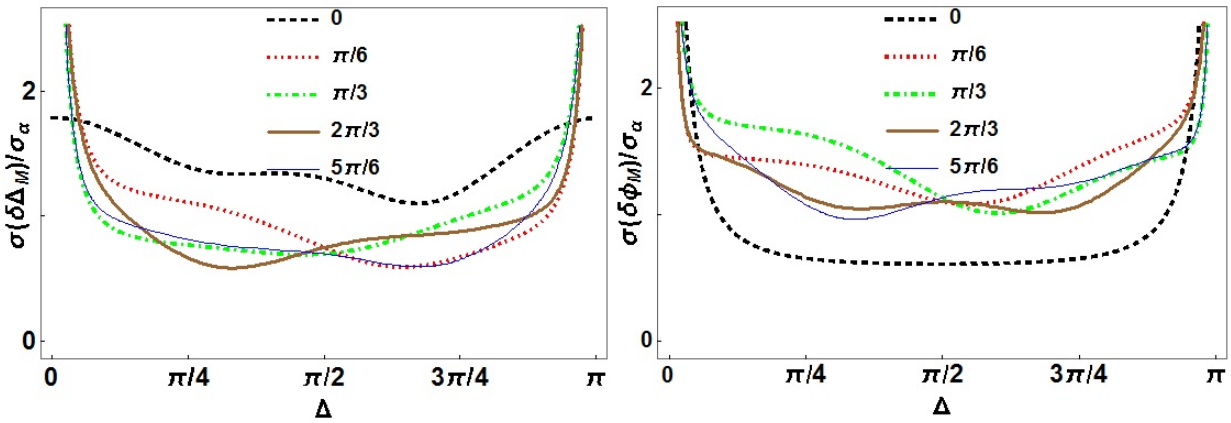

FIG. 4**.** (Color online) Normalized standard deviations $\sigma(\delta\Delta_M)/\sigma_\alpha$ and $\sigma(\delta\phi_M)/\sigma_\alpha$ vs. Δ for different values of ϕ and the set $\boldsymbol{A}=\boldsymbol{A}^{\boldsymbol{B}}$.

We assume that the diagonal elements Ξ_{ii} that determine the relative measurement errors $\delta b_i=\Xi_{ii}b_i$ are identically uniformly distributed random variables $\boldsymbol{\Xi}_{ii}\sim unif\left[-\sqrt{3}\sigma_\Xi,\sqrt{3}\sigma_\Xi\right]$ with standard deviation $\sigma_\Xi=\sigma(\delta\Xi_{ii})$. Then from equation (13), we obtain the standard deviations for the propagated errors $\delta\Delta_B$ and $\delta\phi_B$,

$$\sigma(\delta\Delta_B)=\sigma_\Xi\sqrt{\sum_{i=1}^{4}\left(\frac{\partial\Delta_B}{\partial b_i}b_i\right)^2},\quad \sigma(\delta\phi_B)=\sigma_\Xi\sqrt{\sum_{i=1}^{4}\left(\frac{\partial\phi_B}{\partial b_i}b_i\right)^2} \tag{42}$$

The normalized standard deviations $\sigma(\delta\Delta_M)/\sigma_\Xi$ and $\sigma(\delta\phi_M)/\sigma_\Xi$ are shown in figure 5 as functions of Δ for several fixed values of ϕ for the set $\boldsymbol{A}=\boldsymbol{A}^{\boldsymbol{B}}$.

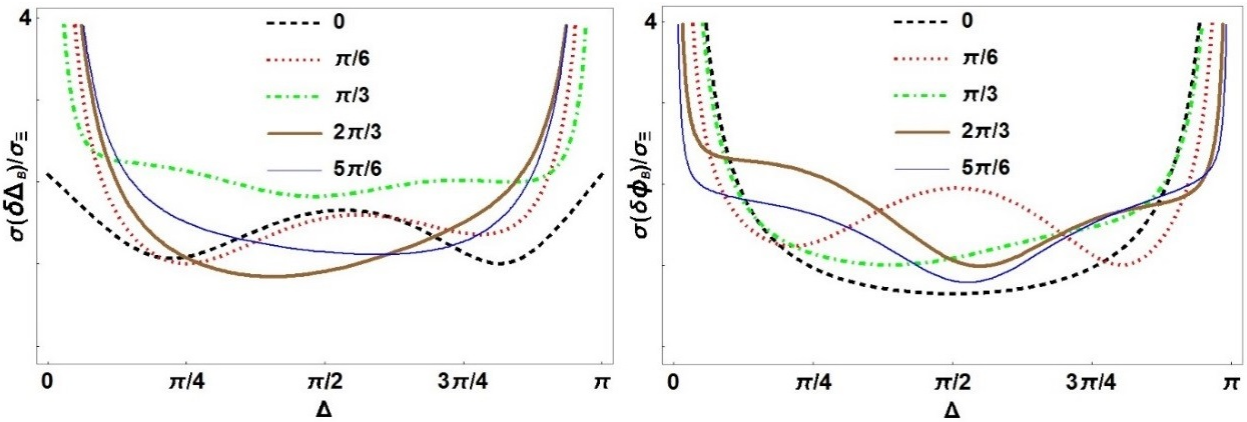

FIG. 5. (Color online) Normalized standard deviations $\sigma(\delta\Delta_B)/\sigma_\Xi$ and $\sigma(\delta\phi_B)/\sigma_\Xi$ vs. Δ for different values of ϕ , set $\boldsymbol{A}=\boldsymbol{A}^{\boldsymbol{B}}$.

For the other sets $\boldsymbol{A}^{\boldsymbol{90}}$, $\boldsymbol{A}^{\boldsymbol{11}}$, and $\boldsymbol{A}^{\boldsymbol{T}}$, the functions (41) and (42) exhibit similar weak dependence on ϕ and strong dependence on Δ. Thus to compare the sets $\boldsymbol{A}^{\boldsymbol{B}}$, $\boldsymbol{A}^{\boldsymbol{90}}$, $\boldsymbol{A}^{\boldsymbol{11}}$, and $\boldsymbol{A}^{\boldsymbol{T}}$, we use the averaged functions over the whole interval of possible values of ϕ, e.g.

$$\overline{\delta\Delta_M}=\frac{1}{\pi\sigma_\alpha}\int_0^\pi\sigma(\delta\Delta_M)\,d\phi \tag{43}$$

and the averaged functions $\overline{\delta\phi_M}$, $\overline{\delta\Delta_B}$, $\overline{\delta\phi_B}$ are defined similarly. Figure 6 demonstrates that the parameter set $\boldsymbol{A}^{\boldsymbol{B}}$ determined by our method provides the smallest values of $\overline{\delta\Delta_M}$, $\overline{\delta\phi_M}$, $\overline{\delta\Delta_B}$, and $\overline{\delta\phi_B}$ in almost the entire range of Δ. Only in the case of small values of retardation Δ, the functions $\overline{\delta\Delta_B}$ and $\overline{\delta\phi_B}$ take the smallest values for the set $\boldsymbol{A}^{\boldsymbol{11}}$, which has been specially designed by Oldenbourg and Schribak to study living cells and other objects with small retardance [4]. Note that the proposed method works well despite the presence of singularities at points $\Delta=0$ and $\Delta=\pi$.

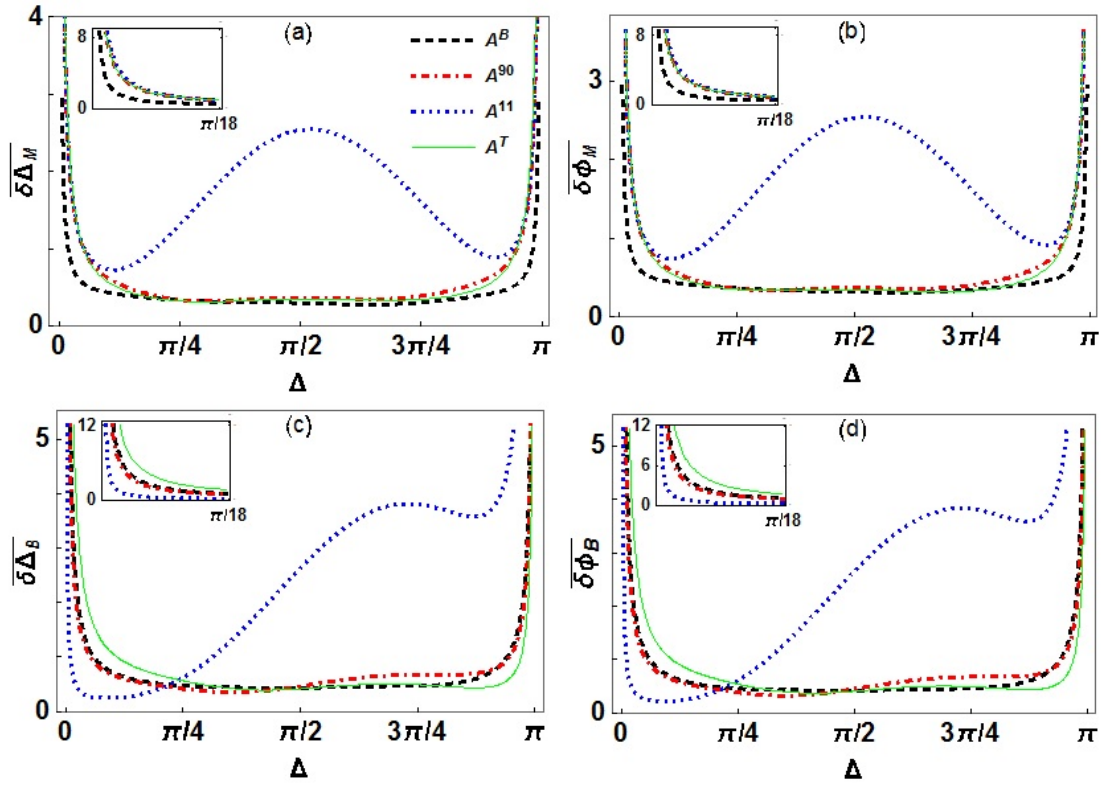

FIG. 6. (Color online) $\phi-$ averaged standard deviations $\overline{\delta\Delta_M}$, $\overline{\delta\phi_M}$, $\overline{\delta\Delta_B}$, $\overline{\delta\phi_B}$ vs. Δ for sets $\boldsymbol{A^B}$, $\boldsymbol{A^{90}}$, $\boldsymbol{A^{11}}$, $\boldsymbol{A^T}$. Inset shows the same plots for small values of $\Delta\in[0,\pi/180]$.

Noise contamination of the measurement process

To illustrate how the selected control parameters affect the measuring accuracy, we numerically simulate the effect of the artificially added noise to the typical PolScope file of a liquid crystal sample, similar to ones presented in [13]. The file contains 2D fields of retardation $\Delta^*(x,y)$, figure 7a, and optical axis orientation $\phi^*(x,y)$, figure 8a, which we consider as the error-free 2D field of quantities $\boldsymbol{\Lambda}^*(x,y)$, assuming that $I_{in}=1$ and $I_{leak}=0$. Then for the selected $\boldsymbol{A}$ we perform the following steps for each pixel (x,y):

(1) We calculate the error-free vector of measured values $\boldsymbol{b}^*=\boldsymbol{M}(\boldsymbol{A})\boldsymbol{V}(\boldsymbol{\Lambda}^*)$.

(2) To simulate effect from errors in control parameters, we contaminate data with artificial noise by adding random, uniformly distributed values $\boldsymbol{\delta A}=\{\delta\alpha_{kj}\}$, $k=1,\ldots,4,\ j=1,\ 2,$

$\delta\alpha_{kj}\sim unif[-3\pi/180,\ 3\pi/180]$ to the set $\boldsymbol{A}$.

(3) We determine the vector $\boldsymbol{V}(\boldsymbol{\Lambda})=[v_1,v_2,v_3,v_4]$ from the equation $\boldsymbol{M}(\boldsymbol{A}+\boldsymbol{\delta A})\boldsymbol{V}(\boldsymbol{\Lambda})=\boldsymbol{b}^*$ via LU decomposition [8] of the matrix $\boldsymbol{M}$ and calculate the retardation $\Delta_M=\cos^{-1}\left(\frac{v_2}{\sqrt{v_2^2+v_3^2+v_4^2}}\right)$ and the orientation of the slow optical axis $\phi_M=\frac{1}{2}\cot^{-1}\left(-\frac{v_3}{v_4}\right)$ contaminated with noise in the control parameters.

(4) We introduce the relative noise of measuring values as $\boldsymbol{\delta b}=\boldsymbol{\Xi b}^*$, where $\boldsymbol{\Xi}$ is a diagonal matrix with identically distributed random elements $\Xi_{ii}\sim unif[-3/100,3/100]$.

(5) We calculate the retardation $\Delta_B=\cos^{-1}\left(\frac{v_2}{\sqrt{v_2^2+v_3^2+v_4^2}}\right)$ and orientation of the slow optical axis $\phi_B=\frac{1}{2}\cot^{-1}\left(-\frac{v_3}{v_4}\right)$ from the equation $\boldsymbol{M}(\boldsymbol{A})\boldsymbol{V}(\boldsymbol{\Lambda})=\boldsymbol{b}^*+\boldsymbol{\delta b}$ similar to step (3).

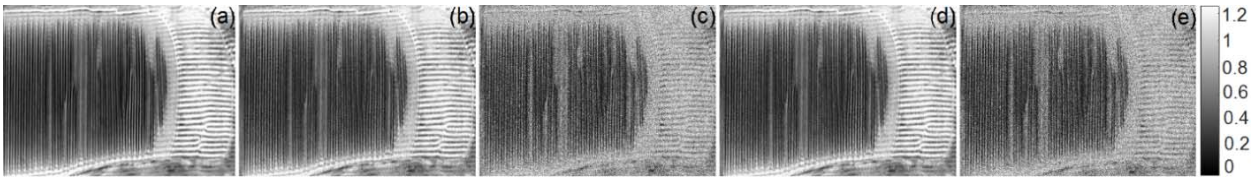

FIG. 7. Effect of noise contamination on retardation: a) original (noise-free) image $\Delta^*(x,y)$; b) image with noise in control parameters $\Delta_M(x,y)$ when $\boldsymbol{A}=\boldsymbol{A^B}$; c) $\Delta_M(x,y)$ when $\boldsymbol{A}=\boldsymbol{A^{90}}$; d) image with relative noise in measured values $\Delta_B(x,y)$ when $\boldsymbol{A}=\boldsymbol{A^B}$; e) $\Delta_B(x,y)$ when $\boldsymbol{A}=\boldsymbol{A^{90}}$. The grayscale bar represents values of the optical retardation.

Figure 7 exhibits the effect of control parameters errors on the retardation for the sets $\boldsymbol{A^B}$ and $\boldsymbol{A^{90}}$ after applying steps (1)-(3) for each pixel. One can see that in comparison with the original error-free image $\Delta^*(x,y)$, figure 7a, the measurement process at $\boldsymbol{A}=\boldsymbol{A^B}$ has a substantially smaller image degradation $\Delta_M(x,y)$, figure 7b, than when $\boldsymbol{A}=\boldsymbol{A^{90}}$, figure 7c. On the other hand, after steps (4)-(5) images with relative measuring errors $\Delta_B(x,y)$ show similar weak degradation for both sets $\boldsymbol{A^B}$ and $\boldsymbol{A^{90}}$, figure 7d and figure 7e, respectively.

To explain the observed image degradation, we computed sample standard deviations of the errors $\delta\Delta_{M,B}(x,y)=\Delta_{M,B}(x,y)-\Delta^*(x,y)$, $s_\Delta^{M,B}=\sqrt{\frac{1}{N-1}\sum_{x,y}\delta\Delta_{M,B}^2(x,y)}$, that equal,

respectively, $s_{\Delta}^{M}=0.09$, $s_{\Delta}^{B}=0.024$ for $\boldsymbol{A}=\boldsymbol{A^{90}}$ and $s_{\Delta}^{M}=0.042$, $s_{\Delta}^{B}=0.023$ for $\boldsymbol{A}=\boldsymbol{A^{B}}$. As we can see, s_{Δ}^{M} is significantly smaller for $\boldsymbol{A^{B}}$ than for $\boldsymbol{A^{90}}$, while s_{Δ}^{B} is almost the same for both sets.

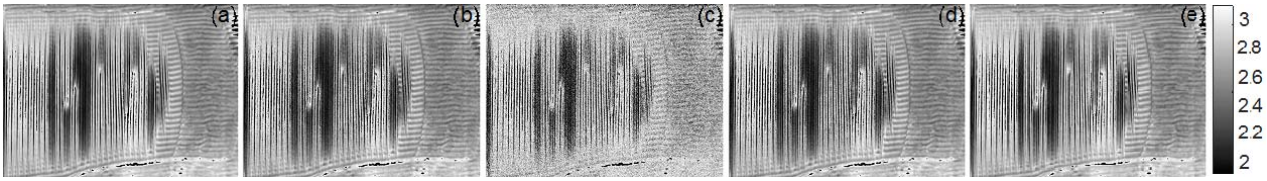

FIG. 8. Effect of noise contamination on the slow axis orientation: a) original (noise-free) image $\phi^{*}(x,y)$; b) image with noise in control parameters $\phi_{M}(x,y)$ when $\boldsymbol{A}=\boldsymbol{A^{B}}$; c) $\phi_{M}(x,y)$ when $\boldsymbol{A}=\boldsymbol{A^{90}}$; d) image with relative noise in measured values $\phi_{B}(x,y)$ when $\boldsymbol{A}=\boldsymbol{A^{B}}$; e) $\phi_{B}(x,y)$ when $\boldsymbol{A}=\boldsymbol{A^{90}}$. The grayscale bar represents values of the slow axis azimuthal angle.

The effect of noise contamination on the optical slow axis orientation data is shown in figure 8. The choice of the set $\boldsymbol{A^{B}}$ leads to smaller image degradation $\phi_{M}(x,y)$, see figure 8b, of the error-free image $\phi^{*}(x,y)$, figure 8a, than the set $\boldsymbol{A^{90}}$, figure 8c. At the same time images with relative noise in the measured values $\phi_{B}(x,y)$ exhibit a similar slight degree of degradation for the sets $\boldsymbol{A^{B}}$ and $\boldsymbol{A^{90}}$, figures 8d and 8e, respectively. The values of sample standard deviations of the slow axis orientation errors, $s_{\phi}^{M,B}=\sqrt{\frac{1}{N-1}\sum_{x,y}\delta\phi_{M,B}^{2}(x,y)}$, where $\delta\phi_{M,B}(x,y)=\phi_{M,B}(x,y)-\phi^{*}(x,y)$, characterize the visual degree of image degradation shown on figure 8, $s_{\phi}^{M}=0.11$, $s_{\phi}^{B}=0.029$ for $\boldsymbol{A}=\boldsymbol{A^{90}}$ and $s_{\Delta}^{M}=0.051$, $s_{\Delta}^{B}=0.027$ for $\boldsymbol{A}=\boldsymbol{A^{B}}$. One can see that the relations between the sample standard deviations s_{Δ}^{M}, s_{ϕ}^{M} , s_{Δ}^{B}, s_{ϕ}^{B} for both sets $\boldsymbol{A^{B}}$, $\boldsymbol{A^{90}}$ match well the relations between the averaged standard deviations $\overline{\delta\Delta_{M}}$, $\overline{\delta\phi_{M}}$, $\overline{\delta\Delta_{B}}$, $\overline{\delta\phi_{B}}$, shown in figures 6a-d.

IV. CONCLUSIONS

In this paper we study the accuracy of CMPMSs to determine several unknown quantities by successively measuring a single physical variable under different experimental conditions,

defined by the control parameters. The errors of the determined quantities are caused by the measurement errors and the errors in the setting of the control parameters. One of the main problems in CMPMSs is the determination of a suitable set of control parameters that provides the best possible accuracy for the entire range of the unknown quantities.

We propose a mathematical method for determination of control parameters for CMPMSs where the measuring function has separable form (2). As an error function, we consider the mathematical expectation of the length of the dimensionless, scaled vector of errors of the unknown quantities (7). The error function splits into two independent functions, describing respectively the effects of the measurement errors and the control parameters errors, (11). Using submultiplicativity of the spectral and Frobenius matrix norms, we represent these two functions as products of factors that dependent only on control parameters and factors that dependent on unknown quantities. Substituting the factors that depend only on the unknown quantities with a weighting coefficient, we construct the effective error function (26), which is the upper bound of the true error function (11). We determine an optimal set of control parameters by minimizing (26).

To demonstrate the capability of our method, we apply it to the PolScope polarized light microscope. In the PolScope, 2D distributions of optical retardation and optical slow axis orientation are determined from four measurements of the light intensity coming through the optical scheme and controlled by variable retarders. We have found that for the PolScope, our method provides almost the same set of control parameters both when minimizing the control parameter error and when minimizing the measuring error, so the optimization of (26) is essentially independent on the weighting coefficient. We compare the computed optimal set of control parameters with other sets including those used in the PolScope and demonstrate that our computed set works very well for the entire range of determined quantities.

The proposed method is applicable to any error distributions of the control parameters and of the measured values, and can be used for optimization of various CMPMSs, in particular, for latest "polarized light microscopy" techniques, Exicor and Polaviz.

ACKNOWLEDGEMENTS

The work was supported by NSF Grants No. DMS-1434185, No. DMS-1729509, and No. DMS-1720259. The authors thank J. Xiang for providing the PolScope file and O. D. Lavrentovich and M. Shribak for fruitful discussions.

References:

[1] S. G. Rabinovich, *Evaluating measurement accuracy : a practical approach* (Springer, New York, 2013).
[2] A. Bjerhammar, *Theory of errors and generalized matrix inverses* (Elsevier, Amsterdam, New York, 1973).
[3] M. Shribak and R. Oldenbourg, Appl. Opt. **42**, 3009 (2003).
[4] R. Oldenbourg, J Microsc-Oxford **231**, 419 (2008).
[5] S. B. Mehta, M. Shribak, and R. Oldenbourg, J Optics-Uk **15**, 094007 (2013).
[6] https://www.hindsinstruments.com/products/exicor.
[7] http://polaviz.com/.
[8] N. J. Higham, *Accuracy and stability of numerical algorithms* (Society for Industrial and Applied Mathematics, Philadelphia, 2002), 2nd edn.
[9] L. N. Trefethen and D. Bau, *Numerical linear algebra* (Society for Industrial and Applied Mathematics, Philadelphia, 1997).
[10] R. Oldenbourg and G. Mei, J Microsc-Oxford **180**, 140 (1995).
[11] B. E. A. Saleh and M. C. Teich, *Fundamentals of photonics* (Wiley, Hoboken, N.J. , 2007).
[12] E. Collett, *Field guide to polarization* (SPIE Press, Bellingham, Wash., 2005).
[13] J. Xiang, S. V. Shiyanovskii, C. T. Imrie, and O. D. Lavrentovich, Phys. Rev. Lett. **112**, 217801 (2014).